05,08

Magnetostatic surface waves losses caused by spin pumping in the ferrite/metal structure

© V.K. Sakharov[1,2], Y.V. Khivintsev[1,2], Y.V. Nikulin[1,2], M.E. Seleznev[1,2], Y.A. Filimonov[1,2]

[1] Saratov Branch, Kotel'nikov Institute of Radio Engineering and Electronics, Russian Academy of Sciences, Saratov, Russia
[2] Saratov National Research State University, Saratov, Russia

E-mail: valentin@sakharov.info

Received April 18, 2024
Revised April 18, 2024
Accepted May 8, 2024

This work presents the results of numerical calculations of magnetostatic surface waves (MSSWs) losses caused by spin pumping mechanism at propagation in a ferrite film covered by a metal with the strong spin-orbit interaction. The calculations were carried out within the framework of known model taking into account the influence of spin pumping on MSSW propagation through the imaginary part of the complex pinning parameter at the ferrite/metal interface. The cases of frequency-dependent and constant pinning parameters are considered and obtained results were compared with the experimental data.

Keywords: spin waves, pinning parameter, propagation losses, yttrium-iron garnet.

DOI: 10.61011/PSS.2024.07.58975.48HH

1. Introduction

The structures made of double-layer films of ferrite-insulator materials and metals [1–6] are now extensively studied for the purpose of design of the data processing, storage and transfer devices where spin waves (SW) or magnons serve as the signal carriers. Typically, yttrium-iron garnet is chosen as a ferrite material with incredibly low SW propagation losses, while platinum is chosen as a metal with strong spin-orbit interaction. In YIG/Pt structures, the conductivity electrons in Pt are sensitive to the state of magnetic ions on the surface of YIG, which results in the spin-dependent electron-magnon scattering and generation of spin current J_S through a unit area of the interface. The spin-Hall and spin transfer torque effects in such structures allow to transform the electric signal into SW and vice versa [2,3], which is important for design of SW detectors [7,8], magnon transistors [9] and magnon memory [10], spin logics devices [1,11], as well as for SW enhancement and generation [12–14].

Theoretical studies of the spectrum of dipole-exchange SW in YIG/Pt structures [4–6] take into account the influence of electron-magnon scattering at the YIG/Pt interface trough the imaginary part Λ'' of the complex pinning parameter $\Lambda = \Lambda' - i\Lambda''$. In this approach, the value Λ'' is assumed proportional to the spin mixing conductance G ($\Lambda'' \sim G$) at interface, which defines the spin current $J_S \sim G$. In addition, SW losses due to introduction of Λ'' are associated with additional SW losses for J_S generation. In works [4–6], the contribution to the temporal SW decrement was calculated which was characterized by an addition $\Delta\omega''(\Lambda'')$ to the imaginary component ω'' of the complex frequency $\omega = \omega' + i\omega''$ associated with the line width of the resonant mode in experiments on spin pumping at conditions of excitation of an uniform FMR [3]. In this work, using the approach [4–6], we consider SW losses at the conditions of spin pumping by propagating magnetostatic surface waves (MSSW). In this case, we consider the contribution $\Delta k''(\Lambda'')$ to the MSSW spatial decrement k'' (imaginary component of the wave number $k = k' + ik''$) as a wave parameter for pumping that determines the J_S generation.

It should be noted that in the spin pumping experiments, we may assess the efficiency of J_S generation based on the EMF generated at the ends of Pt film due to the inverse spin Hall effect (ISHE) V_{ISHE}. For the case of spin pumping by the propagating MSSW in YIG/Pt structures, in the frequency dependence $V_{\mathrm{ISHE}}(\omega)$, the resonant oscillations can be observed at frequencies ω_N of the resonant interaction of the MSSW with the exchange modes of the YIG film [15,16], which can be written in the form [17]:

$$\omega_N = \sqrt{(\omega_H + \omega_{ex,N})(\omega_H + \omega_{ex,N} + \omega_m)}, \qquad (1)$$

where $\omega_H = \gamma H$, $\omega_m = \gamma 4\pi M$, H — external applied field, γ — gyromagnetic ratio, $4\pi M$ — effective saturation magnetization, $\omega_{ex,N} = 2\gamma A_{ex} Q_N^2/M$, $Q_N^2 = k^2 + k_{\perp,N}^2$, $k_{\perp,N} = \pi N/d$ — wave number across the thickness d of YIG film, N — mode number, A_{ex} — exchange stiffness. Since the efficiency of resonant interaction of MSSW with the exchange modes greatly depends on Λ parameter, in this paper, we consider the results of $\Delta k''(\Lambda'')$ calculation for a structure based on YIG film with the parameters close to those in paper [18].

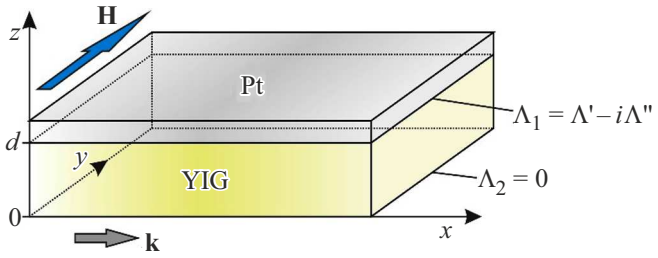

Figure 1. Schematic representation of the studied structure.

2. Methodology of calculation and structure parameters

The considered structure with the coordinate system and the direction of the applied field are shown in Figure 1 Parameters of YIG film were taken as follows: $d = 3.0\,\mu$m, $4\pi M = 1.75$ kG, $A_{ex} = 3.5 \cdot 10^{-7}$ erg/cm, SW damping parameter $\alpha = 3 \cdot 10^{-4}$. The external field $H = 900$ Oe was applied along axis y, while SW propagated along x axis. Such geometry corresponds to MSSW with an amplitude maximum at the Pt/YIG boundary.

The dependencies of dispersions $k'(f)$ and losses $k''(f)$ on frequency f were calculated with the use of approach equivalent to the method described in [20–22]. This approach is based on solving the dispersion equation obtained from the compatibility conditions for the continuity equations for the tangential components of the magnetic field h_x and the normal components of the magnetic induction $b_z = h_z + 4\pi m_z$, as well as boundary conditions for z- and x-magnetization components (m_z, m_x) in the form typical for the normal uniaxial surface anisotropy [23]:

$$\frac{\partial m_z}{\partial z} + \Lambda_1 m_z = 0|_{z=d}; \quad \frac{\partial m_x}{\partial z} = 0|_{z=d}; \qquad (2)$$

$$\frac{\partial m_z}{\partial z} - \Lambda_2 m_z = 0|_{z=0}; \quad \frac{\partial m_x}{\partial z} = 0|_{z=0}, \qquad (3)$$

with substitution of joint solutions of Landau–Lifshitz and the magnetostatics equations in them. Herewith, the components $h_{x,z}(x,z)$, $m_{x,z}(x,z)$ can be represented as a superposition of 6 partial waves with amplitudes B_i [20]:

$$h_{x,z} m_{z,x} \sim \sum_{i=1}^{i=6} B_i e^{k_{z,i} z} e^{i(kx - \omega t)}.$$

Two of these waves are the volume exchange waves with the distribution across the film thickness defined by the wave numbers $k_{z\,1,2} \sim \pm i\pi N/d$. The other four waves have surface character. Two of them correspond to the dipole MSSW with $k_{z\,3,4} = \pm k$. The other two waves are exchange surfaces waves with $k_{z\,5,6} \sim \pm\sqrt{4\pi M^2/A} \approx \pm 10^6\,\text{cm}^{-1}$. In general case, the conditions (2) and (3) take into account the pinning parameters for the surface spins at the boundary with metal (Λ_1) and substrate (Λ_2). To account the losses on the generation of V_{ISHE}, the pinning parameter Λ_1 was introduced in a complex form $(\Lambda_1 = \Lambda = \Lambda' - i\Lambda'')$. On the opposite side of the YIG film, the spins were free $(\Lambda_2 = 0)$.

3. Results and discussion

Figure 2, *a* and *b* illustrates the calculated dependencies $k''(f)$ for the cases of the purely imaginary pinning $(\Lambda = 0 - i \cdot 10^4\,\text{cm}^{-1})$ and pinning with non-zero real part $(\Lambda = 10^4 - i \cdot 10^4\,\text{cm}^{-1})$, respectively. Besides that, the cases of absence of MSSW dissipation ($\alpha = 0$, curves *1*) and typical for YIG dissipation values ($\alpha = 3 \cdot 10^{-4}$, curves *2*), as well as the structures with dissipation but without losses on generation of V_{ISHE} ($\alpha = 3 \cdot 10^{-4}$ and $\Lambda'' = 0$, curves *3*) were considered.

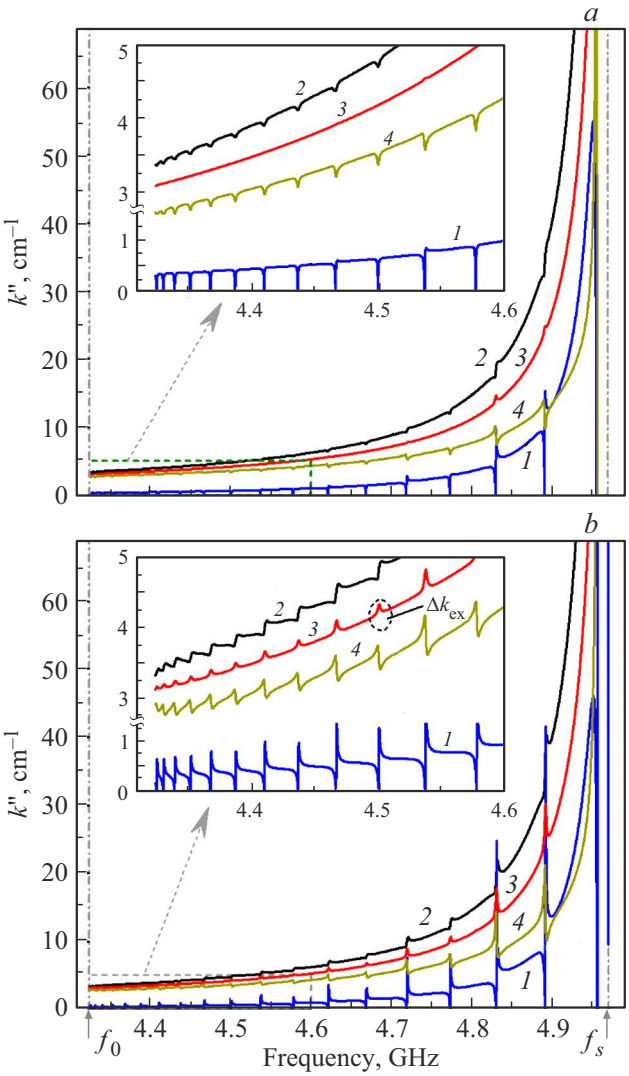

Figure 2. Calculated frequency dependencies of losses $k''(f)$ for the studied structure at (*a*) $\Lambda = 0 - i \cdot 10^4\,\text{cm}^{-1}$ and (*b*) $\Lambda = 10^4 - i \cdot 10^4\,\text{cm}^{-1}$. The curve *1* corresponds to $\alpha = 0$, the curve *2* — $\alpha = 3 \cdot 10^{-4}$, the curve *3* — $\alpha = 3 \cdot 10^{-4}$ and $\Lambda'' = 0$. The curve *4* is equivalent to the curve *2*, but with the change of Λ'' sign. $H = 900$ Oe.

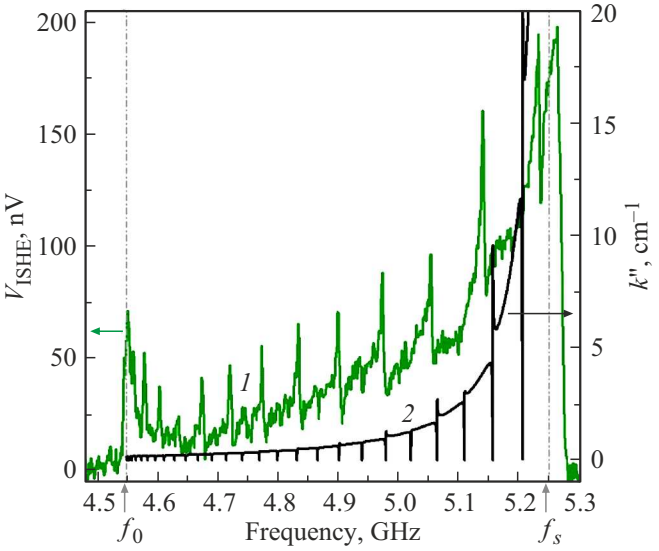

Figure 3. Experimental dependence of EMF of inverse spin Hall effect generated by a MSSW propagating in the YIG(3.9 μm)/Pt(4 nm) structure at the field of 939 Oe (curve *1*) and calculated losses dependence with the same structure parameters (curve *2*).

The obtained curves $k''(f)$ for $\alpha = 0$ and $\Lambda'' \neq 0$ (curves *1*) represent the MSSW attenuation and demonstrate oscillations at frequencies ω_N of dipole-exchange resonances (1). The behavior of curves $k''(f)$ at resonant frequencies significantly depends on the value $\Lambda' = \mathrm{Re}\,(\Lambda)$, which can be seen from the comparison of the curves *1* in Figure 2, *a, b*. In case of $\Lambda' = 0$, at frequencies (1), the curves $k''(f)$ show a dip, followed in some cases by a peak. The non-zero real part of Λ results in formation or increase of this peak formed after the dip in the resonance area. Dissipation of MSSW ($\alpha \neq 0$) leads to the increase of $k''(f)$ values and smoothing of resonance singularities (see curves *1* and *2* in Figure 2, *a, b*). It should be noted that in the considered case, the curves *2* do not represent the exact superposition of curves *1* and *3*, which is especially noticeable for the resonant frequencies near the short-wavelength boundary f_s of MSSW and can be explained by the influence of dissipation on the resonant interaction of MSSW and exchange modes.

The change of sign of Λ'' implies the process inversion — MSSW enhancement due to the spin current in Pt film directed in the opposite side relative to the case considered above [4–6] The calculations for $\Lambda'' < 0$ (curves *4* in Figure 2) demonstrate the reduced losses compared to the situations $\Lambda'' = 0$ (curves *3*) and $\Lambda'' > 0$ (curves *2*), as well as higher oscillations intensity at the frequencies of dipole-exchange resonances and change of their form. With the growth of $|\Lambda''|$ and $\Lambda'' < 0$ one can get a situation when MSSW dissipation losses will be compensated, which for $\alpha = 3 \cdot 10^{-4}$ occurs at $\Lambda'' \approx -2 \cdot 10^5\,\mathrm{cm}^{-1}$. Respectively, at $|\Lambda''| > 2 \cdot 10^5\,\mathrm{cm}^{-1}$ the propagating MSSW will be enhanced (i. e. $k'' < 0$).

Let us compare the calculated MSSW losses for spin current generation with experimental results for the spin pumping with dipole-exchange waves [18] for YIG(3.9 μm)/Pt(4 nm) structure. It is worth to note that the character of dependencies $k''(f)$ shown by curves *1* and *2* in Figure 2 should correspond to the frequency dependence $V_{ISHE}(f)$ observed in the experiment. Figure 3 illustrates comparison of experimental dependence $V_{ISHE}(f)$ with calculation results using parameters corresponding to the experiment. As seen from Figures 2 and 3, the contribution to $k''(f)$, defined by Λ'', near the long-wavelength boundary f_0 of MSSW is orders of magnitude smaller than for the short-wavelength boundary f_s. However, experimental data obtained for YIG(3.9 μm)/Pt(4 nm) structure (see Figure 3) show that curves $V_{ISHE}(f)$ near frequencies f_0 and f_s demonstrate comparable values. The noted discrepancy can be explained by the fact that pinning parameter was considered frequency independent.

To illustrate the character of changes in our calculations of $k''(f, \Lambda'')$, let us consider 2 cases of a frequency dependence for the imaginary component of the parameter $\Lambda'' = \Lambda''(f)$ with increase near f_0. The first case corresponds to the exponential growth near f_0 and has the form:

$$\Lambda'' = \Lambda_0'' + A \cdot \exp\left[-\frac{(f - f_0)^2}{2w^2}\right], \tag{4}$$

where $\Lambda_0'' = 10^4\,\mathrm{cm}^{-1}$ — constant component, A and w — amplitude and width of the peak, respectively, near f_0. The second type of $\Lambda''(f)$ dependence is similar to the change in the density of states for a dipole MSSW [19]:

$$\Lambda'' = \Lambda_0'' + \frac{A}{\sqrt{f^2 - f_0^2}}. \tag{5}$$

The curves $\Lambda'' = \Lambda''(f)$ obtained from expressions (4) and (5) are shown in Figure 4, *a* and *c*, respectively, while dependencies $k''(f)$ calculated on their base at $\alpha = 0$ are given in Figure 4, *b* and *d*. Form (4) for $\Lambda''(f)$ changes the shape of curve $k''(f)$ at the frequencies close to f_0, and, by selecting parameters A and w, the behavior close to the experimental data $V_{ISHE}(f)$ near f_0 can be archived. $\Lambda''(f)$ dependence from expression (5), apart from drastic growth of $k''(f)$ near f_0 results in the increase of $k''(f)$ in the remaining part of the spectrum and is more close to the character of experimental curves $V_{ISHE}(f)$ (Figure 3).

In the calculations considered above, the influence of Platinum on MSSW characteristics was taken into account only via the pinning of spins at the interface. Within this approach, the metal layer conductivity was neglected, which can be reasonable for small metal thicknesses (units of nanometers), which, as a rule, are used in the experiment. Meanwhile, it is a well known fact that thin metallic films may significantly impact the MSSW losses [25–28]. To compare the levels of ohmic losses with MSSW losses for

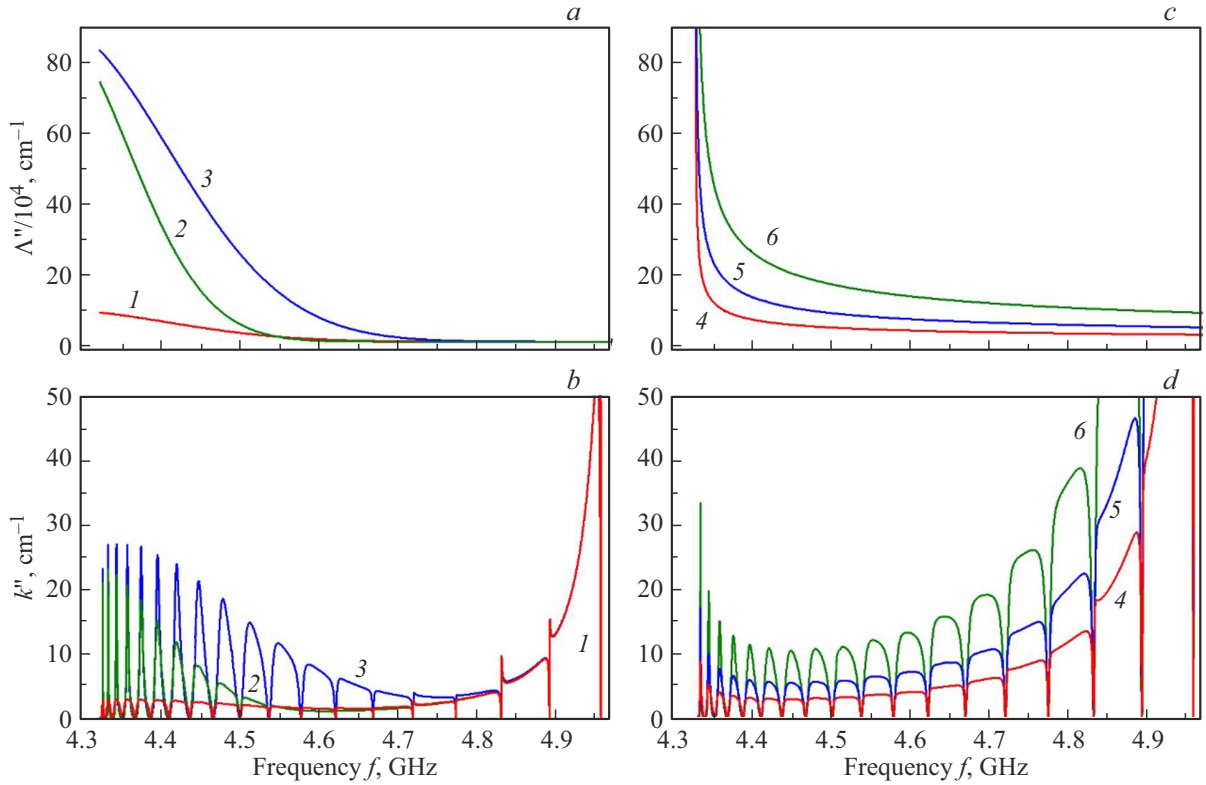

Figure 4. Frequency dependencies of pinning parameters Λ'': (a) — in accordance with the expression (4); (c) — in accordance with the expression (5); and (b, d) — $k''(f)$ curves corresponding to curves in (a) and (c), respectively, for the studied structure.

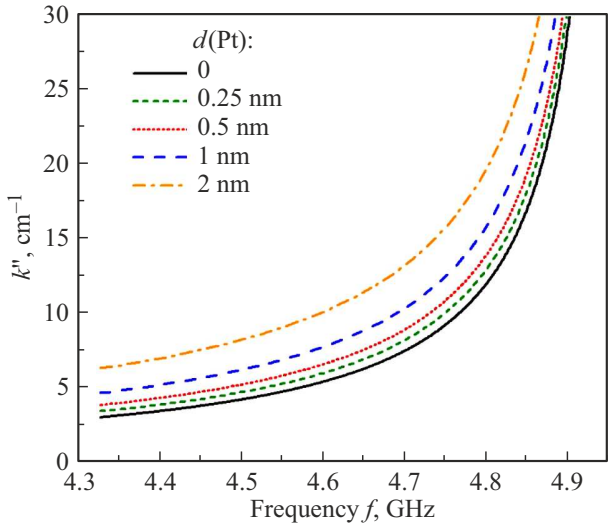

Figure 5. Calculated losses of dipole MSSW due to the metal conductivity at $\alpha = 3 \cdot 10^{-4}$ and different Platinum thicknesses (shown in the figure). $H = 900$ Oe.

spin pumping, we have analyzed the dipole MSSW losses in YIG/Pt structure similar to those in papers [25–28], based on the joint solution of Maxwell and Landau-Lifshitz equations in the non-exchange approximation and neglecting the surface spins pinning.

Figure 5 shows the calculation results of dipole MSSW losses resulting from the finite conductivity of Platinum layer for different metal thicknesses at $\alpha = 3 \cdot 10^{-4}$. Platinum resistivity was taken to be $4 \cdot 10^{-7}\ \Omega \cdot$ m, based on experimental data for $d(\mathrm{Pt}) = 3{-}5$ nm. The calculated curves demonstrate that already at the thickness $d(\mathrm{Pt}) = 0.25$ nm, in the long-wavelength part of the MSSW spectrum, the losses due to metal conductivity (Figure 5) become close to the losses caused by the imaginary component $\Lambda'' = 10^4\ \mathrm{cm}^{-1}$ of pinning parameter (curves *2* in Figure 2) at frequencies outside ω_N. With further growth of Platinum layer thickness, the losses due to conductivity gradually increase and at $d(\mathrm{Pt}) \geq 1.0$ nm, they start to exceed the losses resulting from the spin pinning almost in the entire MSSW range.

4. Conclusion

In this work, we consider a model that describes the losses caused by the generation of EMF of the inverse spin Hall effect at spin pumping by propagating MSSW and is based on the use of a complex spin pinning parameter. It was demonstrated that the calculated losses may correspond to the experimental data if a frequency dependence of pinning parameter $\Lambda''(f)$ is introduced. The losses related to Platinum conductivity begin to exceed the EMF generation losses at the metal thicknesses higher than 1 nm. The

change of sign of the imaginary component of the pinning parameter corresponds to the opposite effect — decrease of MSSW losses because of the spin current in Platinum. For the values of damping parameter $\alpha = 3 \cdot 10^{-4}$, typical for epitaxial YIG films, full compensation of MSSW dissipation is possible at $\Lambda'' \approx -2 \cdot 10^5\,\mathrm{cm}^{-1}$.

Funding

The work has been funded by a grant of the Russian Science Foundation No. 22-19-00500.

Conflict of interest

The authors declare that they have no conflict of interest.

References

[1] K. Ganzhorn, S. Klingler, T. Wimmer, S. Geprägs, R. Gross, H. Huebl, S.T.B. Goennenwein. Appl. Phys. Lett. **109**, 022405 (2016).
[2] Y. Kajiwara, K. Harii, S. Takahashi, J. Ohe, K. Uchida, M. Mizuguchi, H. Umezawa, H. Kawai, K. Ando, K. Takanashi, S. Maekawa, E. Saitoh. Nature **464**, 262 (2010).
[3] S. Maekawa, H. Adachi, K.I. Uchida, J. Ieda, E. Saitoh. J. Phys. Soc. Jpn **82**, 102002 (2013).
[4] J. Xiao, G.E.W. Bauer. Phys. Rev. Lett. **108**, 217204 (2012).
[5] Y. Zhou, H. Jiao, Y.T. Chen, G.E.W. Bauer, J. Xiao. Phys. Rev. B **88**, 184403 (2013).
[6] A. Kapelrud, A. Brataas. Phys. Rev. Lett. **111**, 097602 (2013).
[7] K. Ando, J. Ieda, K. Sasage, S. Takahashi, S. Maekawa, E. Saitoh. Appl. Phys. Lett. **94**, 262505 (2009).
[8] C. Hahn, G. De Loubens, M. Viret, O. Klein, V.V. Naletov, J. Ben Youssef. Phys. Rev. Lett. **111**, 217204 (2013).
[9] L.J. Cornelissen, J. Liu, B.J. Van Wees, R.A. Duine. Phys. Rev. Lett. **120**, 97702 (2018).
[10] C.O. Avci, A. Quindeau, C.F. Pai, M. Mann, L. Caretta, A.S. Tang, M.C. Onbasli, C.A. Ross, G.S.D. Beach. Nature Mater. **16**, 309 (2017).
[11] M. Balinskiy, H. Chiang, D. Gutierrez, A. Khitun. Appl. Phys. Lett. **118**, 242402 (2021).
[12] A. Hamadeh, O. d'Allivy Kelly, C. Hahn, H. Meley, R. Bernard, A.H. Molpeceres, V.V. Naletov, M. Viret, A. Anane, V. Cros, S.O. Demokritov, J.L. Prieto, M. Muñoz, G. de Loubens, O. Klein. Phys. Rev. Lett. **113**, 197203 (2014).
[13] E. Padrón-Hernández, A. Azevedo, S.M. Rezende. Phys. Rev. Lett. **107**, 197203 (2011).
[14] H. Merbouche, B. Divinskiy, D. Gouéré, R. Lebrun, A. El Kanj, V. Cros, P. Bortolotti, A. Anane, S.O. Demokritov, V.E. Demidov. Nature Commun. **15**, 1560 (2023).
[15] R.E. De Wames, T. Wolfram. J. Appl. Phys. **41**, 987 (1970).
[16] Yu.V. Gulyaev, A.S. Bugaev, P.E. Zil'berman, I.A. Ignat'ev, A.G. Konoalov, A.V. Lugovskoi, A.M. Mednikov, B.P. Nam, E.I. Nikolaev // JETP Letters. **30**(9), 600 (1979).
[17] A.G. Gurevich, G.A. Melkov. Magnetization Oscillations and Waves. CRC Press, London. 464 P (1996).
[18] M.E. Seleznev, G.M. Dudko, Y.V. Nikulin, Y.V. Khivintsev, V.K. Sakharov, A.V. Kozhevnikov, S.L. Vysotskii, Y.A. Filimonov. Izvestiya VUZ. Applied Nonlinear Dynamics **32**, 405 (2024).
[19] R.W. Damon, J.R. Eshbach. J. Phys. Chem. Solids **19**, 308 (1961).
[20] Y.A. Filimonov, G.T. Kazakov, S.L. Visotsky, B.P. Nam, A.S. He. J. Magn. Magn. Mater. **131**, 235 (1994).
[21] S.L. Vysotsky, G.T. Kazakov, A.V. Maryakhin, Yu.A. Filimonov, A.S. He. FTT **38**, 407 (1996). (in Russian).
[22] B. Hillebrands. Phys. Rev. B **41**, 530 (1990).
[23] N.M. Salansky, M.Sh. Erukhimov. Fizicheskie svoystva i primenenie magnitnykh plenok. Nauka, Novosibirsk (1975). (in Russian).
[24] M.E. Seleznev, Y.V. Nikulin, Y.V. Khivintsev, S.L. Vysotskii, A.V. Kozhevnikov, V.K. Sakharov, G.M. Dudko, E.S. Pavlov, Y.A. Filimonov. Izvestiya VUZ. Applied Nonlinear Dynamics **30**, 617 (2022).
[25] Yu.A. Filimonov, Yu.V. Khivintsev. J. Comm. Technol. Electron. **47**, 910 (2002).
[26] M. Mruczkiewicz, M. Krawczyk. J. Appl. Phys. **115**, 113909 (2014).
[27] Y.V. Khivintsev, G.M. Dudko, V.K. Sakharov, Y.V. Nikulin, Y.A. Filimonov. Phys. Solid State **61**, 1614 (2019).
[28] V.K. Sakharov, Y.V. Khivintsev, A.S. Dzhumaliev, Y.V. Nikulin, M.E. Seleznev, Y.A. Filimonov. Phys. Solid State. **65**, 1134 (2023).

Translated by T.Zorina